Received: 22 November 2022 | Revised: 27 January 2023 | Accepted: 1 March 2023

DOI: 10.1002/jbio.202200359

RESEARCH ARTICLE

JOURNAL OF BIOPHOTONICS

Digital holographic technique based breast cancer detection using transfer learning method

Leena Thomas[1,2,3] | **M. K. Sheeja**[1,2]

[1]Department of Electronics and Communication Engineering, Sree Chitra Thirunal College of Engineering, Thiruvananthapuram, Kerala, India

[2]APJ Abdul Kalam Technological University, Kerala, India

[3]College of Engineering Kallooppara, Pathanamthitta, Kerala, India

Correspondence
Leena Thomas, Department of Electronics and Communication Engineering, Sree Chitra Thirunal College of Engineering, Thiruvananthapuram, Kerala 695018, India.
Email: leenathomasy@gmail.com

Funding information
Kerala State Council for Science, Technology, and Environment (KSCSTE), Govt. of Kerala

Abstract

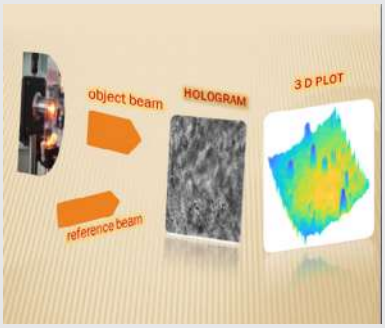

The digital holographic technique is an interferometric method that provides comprehensive information on morphological traits such as cell layer thickness and shape as well as access to biophysical attributes of cells like refractive index, dry mass, and volume. This method helps characterize sample structures in three dimensions both statically and dynamically, even for transparent objects like living biological cells. This research work captures the digital holograms of breast tissues and analyzes the malignancy of the tissue using a deep learning technique. It enables dynamic measurement of the sample under investigation. Different transfer learning models such as Inception, DenseNet, SqueezeNet, VGG, and ResNet are incorporated in this work. The parameters accuracy, precision, sensitivity, and F1 score of different models are compared and found that the ResNet model outperforms better compared to other models.

KEYWORDS

breast tissue, deep learning, digital holography, interferometry, transfer learning

1 | INTRODUCTION

Breast cancer is the most common cancer among women worldwide and the second most common cancer overall [1]. Although it is uncommon in men, it can affect both men and women. According to World Health Organization (WHO) reports, the cancer death ratio is as high as 9.2 million for lung cancer, 1.7 million for skin cancer, and 627 000 for breast cancer [2]. Although early detection and improvements in therapy have enhanced survival rates, it is still the primary cause of mortality among women. The global prevalence of breast cancer cases is expected to cross 2 million by the year 2030. As per the Globocan data 2020 in India, Breast Cancer accounted for 13.5% of all cancer cases and 10.6% of all deaths. There are several types of breast cancer, including ductal carcinoma, lobular carcinoma, inflammatory breast cancer, and triple-negative breast cancer. Staging of breast cancer is done using the TNM method which stands for tumor, node, and metastasis. The decision is made by the size and extent of the tumor, involvement of the lymph nodes, and metastasis to other body regions [3]. Generally, breast tissue can be classified as benign and malignant. A benign tissue is an abnormal but non-cancerous collection of cells in which minor changes in the structure of cells happen and does not pose any threat. Malignant tissue is a cancerous growth that can be dangerous and potentially life-threatening [4].

Conventional assessment of breast cancer is done through the visual examination method under a light

microscope. Manual detection of breast cancer from histopathological images is a big challenge as not all hospitals and clinics have the money and space to appoint a skilled pathologist. The task is tedious, expensive, and time-consuming. Also, over fatigue of pathologists might lead to misdiagnosis. Computer-aided diagnosis (CAD) plays a vital role in overcoming the above-said issues. The current imaging modalities used for the detection of breast cancer include ultrasound, mammography, magnetic resonance imaging (MRI), phase contrast microscopy, infrared spectroscopy, ultrasonography (USG), etc., and all have their pros and cons. Even though these imaging methods are used to detect breast abnormalities and suspicious lesions, a histopathological examination, that is, a biopsy is needed to confirm the diagnosis of breast cancer. CAD can help to identify areas of concern within the images that may be indicative of disease or abnormality and help to improve the accuracy and efficiency of the diagnostic process [5, 6].

The purpose of this research work is to develop an automated system that can quickly and accurately diagnose breast cancer using the digital holographic (DH) method to evaluate the deformation of benign and malignant tissue. DH employs the two-beam configuration technique for the phase imaging of microscopic objects like red blood corpuscles (RBCs), white blood corpuscles (WBCs), platelets, etc. [7]. The charge coupled device (CCD) or the complementary metal-oxide-semiconductor (CMOS) records the amplitude and phase information of the object using a camera in the form of interference fringes called the hologram. The information is then extracted from the digitally recorded holograms using numerical reconstruction methods [7]. Research works done previously have demonstrated that one of the best imaging modalities for examining biological material is DH [8, 9]. The advantage of two beam configuration technique is that it allows the recording of the wide field of view (FOV) of the sample being processed. Also, the two-beam configuration enables have wider angular tilt between the object and reference beams thus preventing the overlap of dc and cross terms in the Fourier domain [10]. However even if the dc and the cross terms of the hologram overlap in the Fourier domain, it is possible for capturing a high-quality image with the Mach-Zehnder interferometer-based DH techniques. In this configuration, the coherent laser beam is split into two beams using a beam splitter, one part lights up the object, while the other is kept unaltered. These two beams are directed in two different directions by the beam splitter. These beams are then combined as a single beam of light by the beam combiner producing interference fringes on CCD. This technique of separation of a single beam into two separate beams leads to reduced temporal phase stability which results in the fluctuations of the phase of an object over time.

Deep learning can be employed for the diagnosis of disease and its subsequent classification based on medical images [11–15]. Deep learning requires a lot of labeled data; however, the size of such medical image datasets is generally limited. Thus transfer learning methods can be incorporated to achieve the classification [16, 17]. The implemented work proposes an alternative method of disease detection and classification with small datasets using deep learning models. The properties of DH increase the arduous nature of modeling the image formation process. The misreading of jumps in the wrapped phase of the image is also an intricate hurdle in holographic image processing. Hence, deep neural networks (DNN) can analyze and operate complex values and the cyclical nature of phases.

In this research work, a deep learning approach for breast cancer tissue classification and disease diagnosis is carried out using an off-axis digital holographic system. The features from a transfer learning pre-trained convolutional neural network (CNN) is extracted for performing the classification. The proposed work provides significant classification accuracy and is the foremost report on deep learning techniques about digital holography towards the diagnosis of breast cancer classification. The rest of the paper is organized as follows: Section 2 describes the existing works carried out in breast cancer detection. The digital holographic imaging system for data collection of benign and malignant tissue and the transfer learning techniques employed are included in Section 3. Section 4 deals with the experimental set-up and results obtained from it and it is followed by discussions and conclusions in Section 5.

The key contributions of this work can be listed as follows.

i. Designing DH system and capturing hologram of breast tissues.
ii. Annotating the data for benign and malignant tissue.
iii. Creating custom dataset of breast hologram.
iv. Developing a deep learning algorithm to classify the hologram tissue.

2 | RELATED WORKS

This section encompasses an overview of the methods utilized by other researchers in their studies. The methods for diagnosing breast cancer have been researched for over four decades, resulting in significant achievements in the field. Research has been conducted using various imaging techniques such as ultrasound,

mammography, histopathology, and MRI for the detection of breast cancer. Machine learning and deep learning techniques along with various feature-extracting algorithms have been applied to these imaging modalities to improve the accuracy of breast cancer detection. Additionally, research has been conducted to understand the genetic and molecular mechanisms of breast cancer, which has led to the development of targeted therapies for the disease. Studies on lifestyle factors, such as diet and physical activity, have also been conducted to understand their potential impact on breast cancer risk and outcomes. Araujo et al. demonstrated the classification of hematoxylin and eosin-stained breast biopsy images using convolutional neural networks. The dataset used were images from the Bioimaging 2015 breast histology classification challenge [4]. The system was designed such that nuclei and overall tissue organization were considered. The features from CNN are given to an SVM classifier. The accuracy observed is 77% with a sensitivity of 95.6%. Wells et al. aim to use phase contrast microscopy to identify differences in the microarchitecture of benign and malignant breast tissue. The histopathological study found that malignant epithelium had significantly higher levels of disorder and disorganization compared to the benign epithelium and that the stroma in malignant tissue was also more disordered and exhibited more mitotic activity [18]. The study observed a sensitivity of 69% and a specificity of 85%. Present the development and validation of a deep learning model for the segmentation and characterization of breast lesions in multiparametric MRI. The model is based on a 3D CNN architecture and is trained and tested on a dataset of patients with breast lesions [19]. The results show that the model can accurately segment and classify breast lesions in multiparametric MRI with a high degree of precision and recall. The accuracy of their model is 84.6% with AUC 92.7.

Kundale et al. present a method for classifying breast cancer using histology images, with a focus on comparing the performance of handcrafted features and pre-trained features [20]. The features are extracted using SURF and DSIFT and these features are used to train a classifier and compare the performance of the classifier using handcrafted features to the performance using pre-trained features and achieve an accuracy of 94%. Azevedo et al. performed a quantum approach to a machine-learning problem. Different popular datasets of mammograms were taken and extracted regions of interest (ROIs) were to perform ML and DL techniques. This technique was found to have an accuracy of 84%, and better specificity and sensitivity compared to existing methods [21]. Reshma et al. utilized breast cancer histological database (BreaKHis) dataset for the study. Here genetic algorithm with convolutional neural network was proposed. Comparing the performance of the genetic algorithm with other feature selection techniques, the genetic algorithm outperforms the competition. The performance of SURF and GLCM feature extraction was evaluated for different classifiers like kNN, Naïve Bayes, SVM, and proposed one [22]. The presented work had an accuracy 94.2% and a precision 86.9%. Ali et al. performed computer-aided diagnosis of multimodal images of breast cancer. In this work machine learning and deep convolutional neural network ResNet50 were employed. Patches of the image were also taken into consideration [23]. The principal component analysis model and linear discriminant analysis (PCA-LDA) were utilized to reduce the high dimensionality of the feature measured and to differentiate between the tissue patches. The sensitivity achieved is 86.2% [24]. Proposed a novel integrated deep learning model, a multi-view deep neural network support vector machine, to achieve breast cancer diagnosis on bi-modal ultrasound images. Guo et al. proposed a classification of histopathology images. Hybrid convolutional neural network (CNN) architecture with GoogLeNet and bagging technique and hierarchy voting method were introduced and the accuracy of the method is 87.5% for four classes [25]. A novel deep hybrid attention approach to breast cancer classification from histopathological images [26]. The public dataset BreakHis is taken for analysis. The hard-attention mechanism in the network could automatically find the useful region from the raw image and thus does not have to resize the raw image for the network to prevent information loss. The built-in recurrent network can make decisions to classify the image and also predict region for the next time step.

3 | METHODOLOGY

3.1 | Off-axis digital holographic set-up for data collection

The breast tissue histopathologic slides have been collected for data preparation. The post-operative collected specimen is immediately fixed in a leak-proof tight jar containing 10% formalin. This prevents autolysis and putrefaction of tissues. After 24–48 h the specimen becomes adequately fixed. It is then cut into thin slices approximately 4 mm thick and each slice is fixed into a cassette which is a high-density polymer case used for storing slides in solutions. The cassette is then again stored in formalin. Subsequently, the tissue is processed in three steps (a) the tissue is then dehydrated by immersing in alcohol to remove formalin and water, (b) the second step involves clearing by adding xylene to

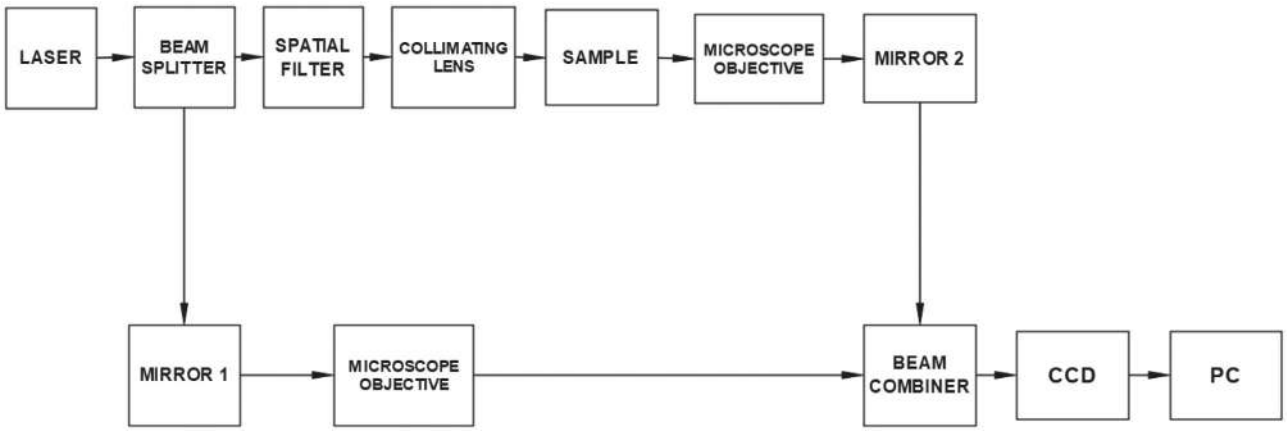

FIGURE 1 Block diagram of off-axis digital holographic set-up.

remove the alcohol. (c) The final step is embedding the specimen by fixing it in a paraffin block. The paraffin block is cut into thin microscopic sections using a microtome and fixed on a glass slide. Most cells are colorless and transparent if unstained. The collected breast tissue samples are then imaged with a DH set-up.

The research work is meant to classify the hologram of a microscopic tissue sample as benign or malignant. The data is prepared using an off-axis digital holographic set-up, and the block diagram of the set-up is shown in Figure 1.

The principle of superposition of two electromagnetic waves is used to extract information within the sample tissue. It produces interference patterns that contain optical path length differences between the two wavefronts and are recorded on a CCD [7]. The main component of this set-up is a 5 mW continuous He–Ne laser of wavelength 632.8 nm. The laser beam is split into two beams with the help of a beam splitter (BS) namely, the object beam and the reference beam. The object beam is then passed through a spatial filter (SF). The SF is used to eliminate high-frequency fluctuations and to get a clear expanded laser beam. A collimating lens (CL) of 100 mm focal length is used to collimate the beam coming from SF and is made to fall on the sample. The microscopic breast tissue is placed as the sample, and a microscopic objective (MO) 20× with a numerical aperture of 0.4 is used to magnify the microscopic tissue. The diffracted object beam carries the structural details of the breast tissue such as refractive index, birefringence and thickness. The diffracted object beam and the reference beam are combined to form an interference pattern using a beam combiner (BS2) with the help of mirror MIRROR2 and are made to fall on the CCD camera (1024 × 1024 pixels), and a digital hologram is recorded. The mirrors and BS are 150 mm in diameter. The mirrors are coated with 99.9% pure silver and have silicon dioxide coating as a protective layer against oxidation. The captured hologram contains fringe patterns which resemble the morphological and optical features of the tissue, such as shape, size, refractive index distributions, and orientation for the incident beam. The digitized hologram is stored on a computer. The schematic of the optical set-up for acquiring the digital hologram of breast tissue is shown in Figure 2.

Mathematically, an object beam $O(x,y)$ and reference beam $R(x,y)$ with complex amplitudes can be expressed as

$$O(x,y) = a(x,y)e^{j\theta(x,y)} \tag{1}$$

$$R(x,y) = b(x,y)e^{j\emptyset(x,y)} \tag{2}$$

where (x,y) are the pixel position in the hologram plane, $a(x,y)$ and $b(x,y)$ are the amplitudes of object wave and reference wave, and $\exp[j\theta(x,y)]$ and $\exp[j\emptyset(x,y)]$ are the phase of object beam, reference beam, etc.

The hologram captured by the CCD camera is given by

$$H(x,y) = |O(x,y) + R(x,y)|^2$$

$$= |O(x,y)|^2 + |R(x,y)|^2 + O^*(x,y)R(x,y) + O(x,y)R^*(x,y) \tag{3}$$

where * represents the complex conjugate. The first two parts are the zero-order terms, while the third and fourth terms are the interference.

The Numerical Reconstruction is to process the hologram to obtain the object information. Numerical reconstruction is performed using the Fresnel transform method. The complex amplitude of the object $\tilde{O}(x,y)$ is

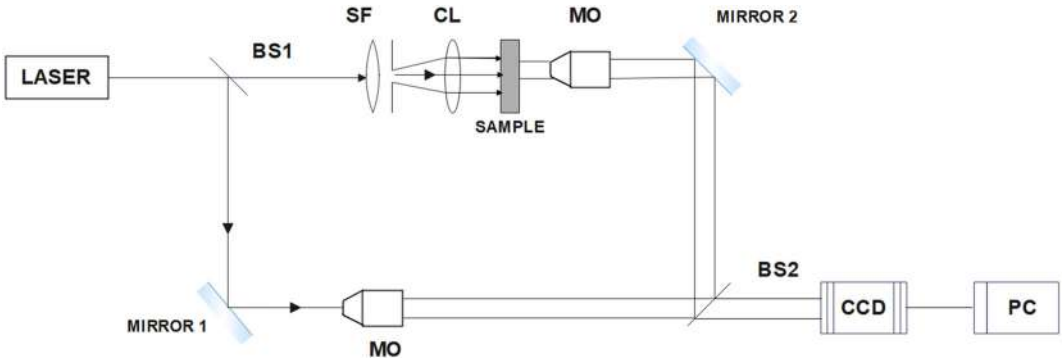

FIGURE 2 Schematic diagram for digital hologram recording.

$$\tilde{O}(x,y) = F^{-1}[F[H(x,y)R(x,y)]F[h(\varepsilon,\eta,x,y)]] \quad (4)$$

where ε,η indicates the sampling interval, $\varepsilon = \frac{\lambda d}{Nx}$ and $\eta = \frac{\lambda d}{Ny}$, is the wavelength of laser source, N is number of pixels of camera, d is the distance between object plane and image plane and $h(\varepsilon,\eta,x,y)$ represents the impulse response function.

The reconstructed amplitude image is

$$\tilde{o}(x,y) = \mathrm{Re}\left[\tilde{O}(x,y)\right]^2 + \mathrm{Im}\left[\tilde{O}(x,y)\right]^2 \quad (5)$$

The reconstructed phase image is

$$\theta(x,y) = \arctan\frac{\mathrm{Im}\left[\tilde{O}(x,y)\right]}{\mathrm{Re}\left[\tilde{O}(x,y)\right]} \quad (6)$$

The complicated nature of digital holography increases the travail in modeling an image formation step. However, deep neural networks are expected to handle these problems efficiently. The captured holograms are quite huge and contain a lot of data. Thus deep learning algorithms with transfer learning will help to exploit the information present in the image. The goal is to use deep learning techniques to extract spatial, spectral, and phase information from the wavefront of an object recorded in a hologram.

Deep learning techniques are being used for extracting the features of the tissue and thereby performing the detection and classification of breast cancer disease. The classification can be accomplished by incorporating transfer learning techniques. This work suggests a novel training approach for developing disease detection and classification of deep learning models on minimal datasets. The overall proposed architecture for breast cancer diagnosis is illustrated in Figure 3.

Once the data is acquired, data annotation is carried out. In data annotation, data is labeled as benign and malignant. Following the annotation is data pre-processing. In pre-processing each hologram image is converted to 224 × 224 pixels. The data augmentation techniques like scaling, flipping, rotation, and affine transformation are applied. Data augmentation is carried out to enlarge the dataset to alleviate the problem of limited data size. These methods of augmentation aid in overcoming the problem of overfitting in neural networks. The regularization method used in this work is the drop out method.

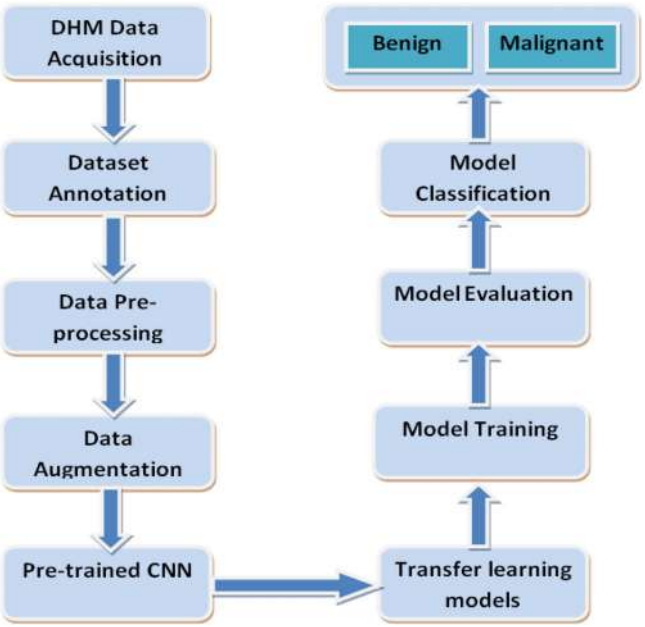

FIGURE 3 Flow diagram of breast cancer diagnosis process.

The CNN models such as Inception, SqueezeNet, DenseNet, VGG, and ResNet, are used in this work to perform the diagnosis of disease. The features present in the hologram image are extracted by the convolution layers present in CNN. The size of the network is reduced by the pooling layers. Backpropagation calculates the gradient of neural network parameters and by which it updates the weight to minimize the loss function. Batch normalization is used, which standardizes and

normalizes operations on the input of a layer coming from a previous layer and ultimately makes the neural network faster and more stable.

3.2 | Evaluation metrics

The overall interpretation of the research model is assessed based on the elements of the confusion matrix. This evaluation matrix contains four terms, namely, true positive (TP), false positive (FP), false negative (FN), and true negative (TN). TP refers to those images that were correctly classified as malignant and the FP represents the benign images mistakenly classified as malignant whereas the FN represents the images belonging to the malignant class that was classified as benign, and the TN refers to the benign images correctly classified. The classification performance of this research model is evaluated using four confusion matrix-based performance measures, which are precision, sensitivity, overall accuracy, and F1 score. These performance measures are calculated as follows:

1. Precision:

$$\text{Precision} = \frac{\text{TP}}{\text{TP} + \text{FP}} \tag{7}$$

2. Sensitivity:

$$\text{Sensitivity} = \frac{\text{TP}}{\text{TP} + \text{FN}} \tag{8}$$

3. Accuracy:

$$\text{Accuracy} = \frac{\text{TP} + \text{TN}}{\text{TP} + \text{TN} + \text{FP} + \text{FN}} \tag{9}$$

4. F1 score:

$$\text{F1 score} = \frac{2 \times \text{Precision} \times \text{Recall}}{\text{Precision} + \text{Recall}} \tag{10}$$

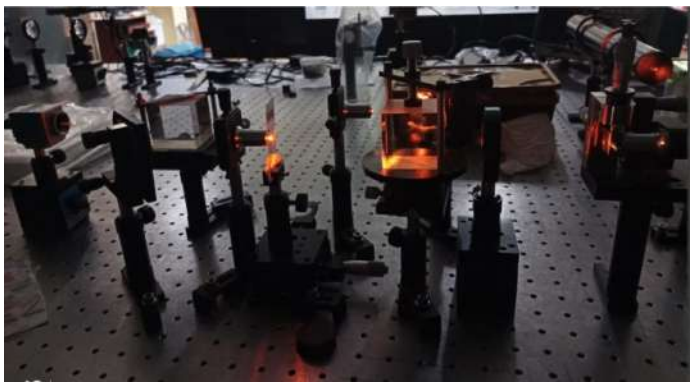

FIGURE 4 Experimental set-up for digital hologram imaging.

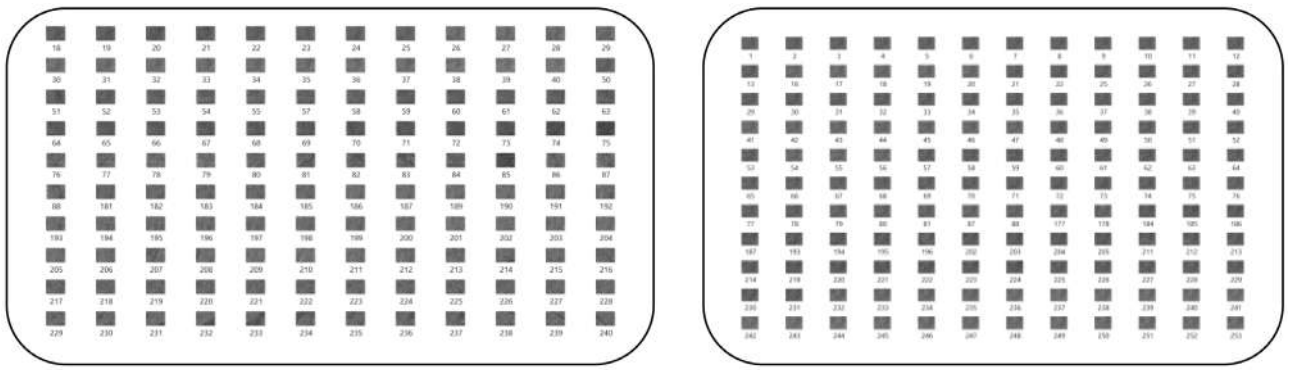

(a) Benign breast tissue hologram (b) Malignant breast tissue hologram

FIGURE 5 Sample dataset of (A) benign breast tissue hologram and (B) malignant breast tissue hologram.

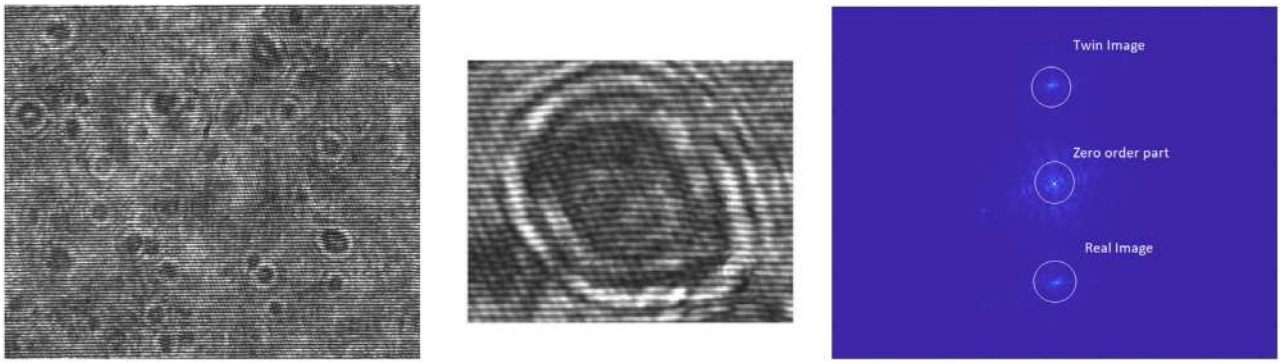

FIGURE 6 (A) Malignant breast tissue hologram, (B) cropped single nucleus, and (C) FFT of cropped nucleus.

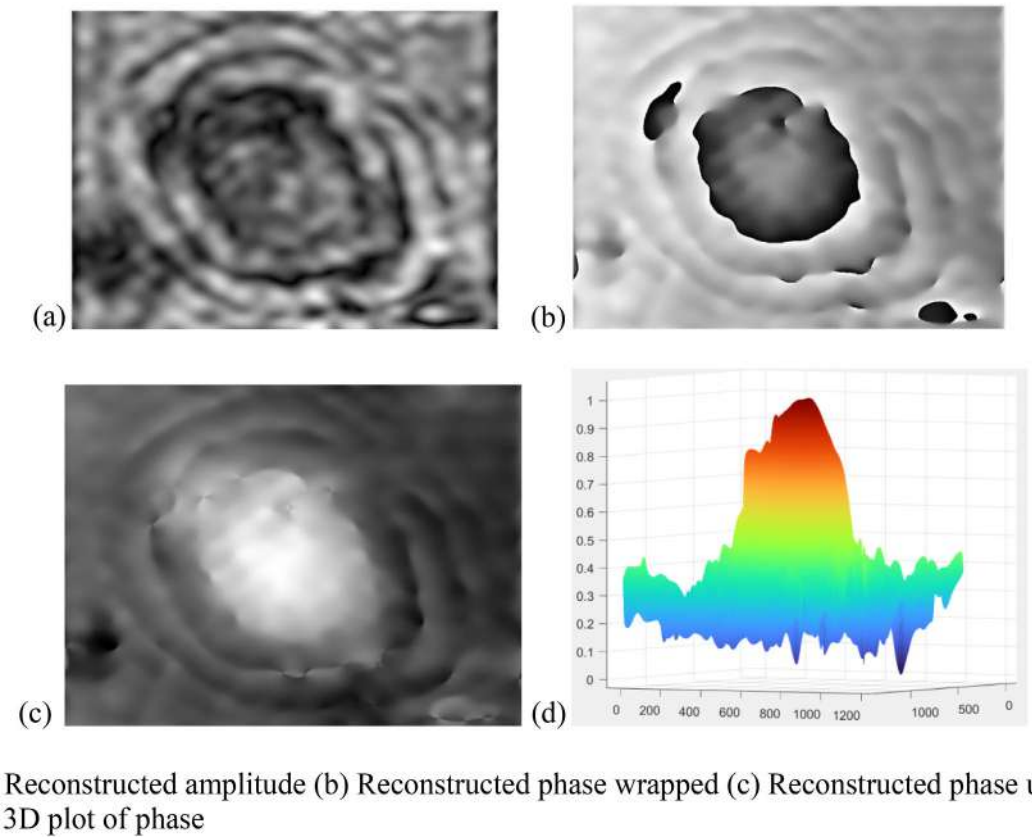

FIGURE 7 (A) Reconstructed amplitude, (B) reconstructed phase wrapped, (C) reconstructed phase unwrapped, and (D) 3D plot of phase.

4 | EXPERIMENTAL RESULTS

The breast tissues were prepared on a microscopic slide and covered by a cover slip and imaged using the off-axis DH method. From 50 slides of benign and 60 slides of malignant tissue, 522 benign holograms and 746 malignant holograms were captured respectively by imaging different areas of histopathological tissue slides. The experimental set-up used for imaging digital holograms of breast tissues is shown in Figure 4. Once the holograms were captured, the dataset was labeled as benign and malignant images. The dataset comprises 1526 hologram images, of which 522 are benign, and 746 are malignant images. The sample dataset of benign and malignant images is shown in Figure 5. The dataset of the digital holograms is divided into the training set, and

test set in the ratio of 70% and 30% respectively. Through the accurate classification of test set images, unknown tissue samples can be correctly identified and detected. The accuracy of the classification of unknown samples is discussed below.

TABLE 1 Confusion matrix of inception model.

	Inception	
	Benign	**Malignant**
Actual		
Benign	328 (TN)	50 (FP)
Malignant	70 (FN)	452 (TP)
	Predicted	

TABLE 2 Confusion matrix of different pre-trained models.

	Squeezenet [1]		Densenet	
	Benign	**Malignant**	**Benign**	**Malignant**
Benign	338	40	346	32
Malignant	50	472	42	480

TABLE 3 Confusion matrix of different pre-trained models.

	VGG19		Resnet	
	Benign	**Malignant**	**Benign**	**Malignant**
Benign	354	24	357	21
Malignant	34	488	30	492

The benign and malignant breast tissues are different in structural components and behavior. The fringe pattern observed in the hologram holds the phase difference between the object beam and the reference beam. The shape and size of the cells are vivid in the fringe patterns of the captured hologram and this is utilized for the distinction of benign and malignant tissues. Figure 6 illustrates the captured hologram of malignant tissue, with (A) showing the entire image and (B) showing a single nucleus that has been cropped from the captured hologram. Figure 6C presents the fast Fourier transform (FFT) of the image shown in Figure 6B. The frequency spectrum of the hologram contains the zero-order term, real image and twin image. The real image is extracted from the three terms by spatial filtering in the frequency domain. Figure 7 displays the reconstructed images, with (A) showing the amplitude image and (B) showing the wrapped phase image. The unwrapped phase image is presented in Figure 7C and a 3D plot of the phase image of a single cropped nucleus is shown in Figure 7D.

The coding was performed in an i5 8GB system on python. Pytorch deep learning framework was used. Here different pre-trained models such as Inception, SqueezeNet, DenseNet, VGG, and ResNet were taken to check the generalization of this framework. The features of transfer learning techniques very well distinguish and classifies the breast tissues. The confusion matrices of different pre-trained models were provided in Table 1,

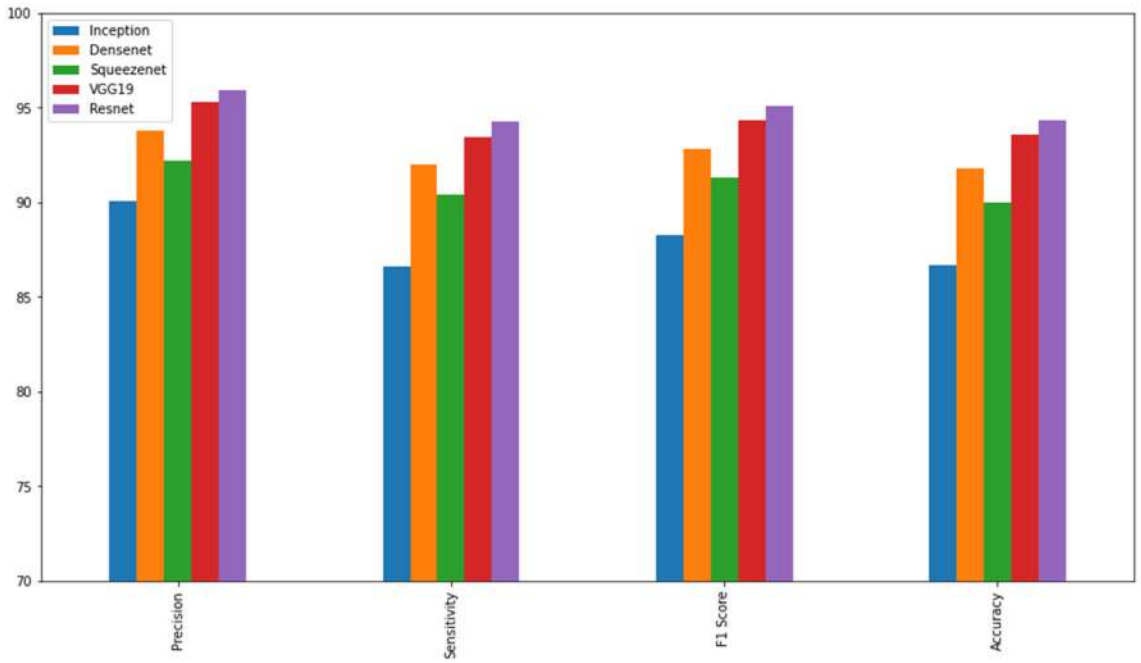

FIGURE 8 Precision, sensitivity, F1 score, and accuracy of different pre-trained models.

Table 2, and Table 3. As in Table 1, for the Inception model, 328 actual benign images are predicted as benign, that is TN. Fifty benign images are mistakenly classified as malignant images, that is, FP. Seventy malignant images are predicted as benign, that is, FN. Four hundred and fifty two malignant images are predicted as malignant. The precision, sensitivity, F1 score, and accuracy plots of different pre-trained models are calculated based on TN, TP, FP, and FN values and are plotted in Figure 8. The precision, sensitivity, F1 score, and accuracy values of Resnet model are 95.9%, 94.25%, 95.068%, and 94.33%, respectively.

5 | DISCUSSIONS AND CONCLUSION

In this research work, the classification of benign and malignant breast tissues is implemented using an off-axis digital holographic system and deep learning technology. Here a new hologram dataset of breast tissues is presented. The creation of an annotated dataset is both a crucial and time-consuming task. Previous studies reported the use of various imaging modalities for the identification of breast cancer. The purpose of the work is to provide a more precise and effective detection method utilizing an automated approach that can help pathologists avoid being overworked and subsequently minimize misinterpretation of results. This attempts to improve patient outcomes by swiftly identifying high-risk individuals for specific illnesses and lowering mortality rates by detecting the disease in its early stage. This may enable early treatments and therapy that is tailored to each patient, increasing the chance of recovery and lowering the risk of complications.

The digital holographic method provides the morphological and phase features of the breast tissue sample. The deep learning technology helps to automatically extract relevant features from the image. The transfer learning models such as Inception, SqueezeNet, DenseNet, VGG, and ResNet applied in this work very well help in the classification of tissues. The classification results show that the research work provides better performance for the detection and identification of breast cancer. The focusing of the image in the focal plane needs to be carried out carefully. Classification accuracy can be improved with larger datasets. The elapsed time for the experiment was around 20 min. The results for the experiments are computed in terms of precision, recall, F1 score, and accuracy. Among the transfer learning models, the ResNet model is observed with a better accuracy of 94.3% and a computation time of 18 minutes. DH is a powerful tool for label-free cell imaging and analysis, offering high-resolution, 3D images and quantitative phase information without the need for staining or other labeling methods. Future studies should focus on label-free microscopic cell analysis.

ACKNOWLEDGMENTS

Partial financial support provided by the Kerala State Council for Science, Technology, and Environment (KSCSTE), Govt. of Kerala is thankfully recognized. Technical support from IIST (Indian Institute of Space Science and Technology) is also thankfully acknowledged.

CONFLICT OF INTEREST STATEMENT

The authors declare no conflicts of interest.

DATA AVAILABILITY STATEMENT

Data available on request due to privacy/ethical restrictions.

ORCID

Leena Thomas https://orcid.org/0000-0003-4511-6421

REFERENCES

[1] X. Zhou, C. Li, M. M. Rahaman, Y. Yao, S. Ai, C. Sun, X. Li, Q. Wang, T. Jiang, *IEEE Access*, *8*, 90931.
[2] GBD 2019 Risk Factors Collaborators, *The Lancet* **2020**, *396*, 1223.
[3] G. D. Z. Anastasiadi, E. Lianos, H. V. Ignatiadou, *M. Updat. Surg.* **2017**, *69*, 313.
[4] S. Reis, P. Gazinska, J. H. Hipwell, T. Mertzanidou, K. Naidoo, N. Williams, S. Pinder, D. J. Hawkes, *IEEE Trans. Biomed. Eng.* **2017**, *64*, 2344.
[5] T. O'Connor, A. Anand, B. Andemariam, B. Javidi, *Optics Express* **2020**, *11*, 4491.
[6] X. He, C. V. Nguyen, M. Pratap, Y. Zheng, Y. Wang, D. R. Nisbet, R. J. Williams, M. Rug, A. G. Maier, W. M. Lee, *Biomed. Optics Exp.* **2016**, *7*, 3111.
[7] D. Jianglei, W. Ji, W. Kaiqiang, T. Ju, L. Ying, Z. Jianlin, *Frontiers Phys.* **2021**, 9.
[8] B. Javidi, A. Markman, S. Rawat, T. O'Connor, A. Anand, B. Andemariam, *Optics Exp.* **2018**, *26*, 13614.
[9] J. Mangal, R. Monga, S. R. Mathur, A. K. Dinda, J. Joseph, S. Ahlawat, K. Khare, *J. Biophotonics* **2019**, 12.
[10] Y. R. He, S. He, M. E. Kandel, Y. J. Lee, C. Hu, N. Sobh, M. A. Anastasio, G. Popescu, *ACS Photonics* **2022**, *9*, 1264.
[11] J. Zhu, J. Geng, W. Shan, B. Zhang, H. Shen, X. Dong, M. Liu, X. Li, L. Cheng, *Front. Ongol*. **2022**, *12*, 946580.
[12] T. Araújo, G. Aresta, E. Castro, J. Rouco, P. Aguiar, C. Eloy, A. Polónia, A. Campilho, *PLoS One* **2017**. https://doi.org/10.1371/journal.pone.0177544
[13] J. Kundale, S. Dhage, *IOP Conf. Series: Mater. Sci. Eng.* **2017**, *1074*, 012008.
[14] V. Azevedo, C. Silva, I. Dutra, *Quantum Machine Intelligence* **2022**, 4.
[15] V. K. Reshma, N. Arya, S. S. Ahmad, I. Watter, S. Mekala, S. Joshi, D. Krah, *Bio Med Res. Int.* **2022**, 363850.
[16] N. Ali, E. Quansah, K. Köhler, T. Meyer, M. Schmitt, J. Popp, A. Niendorf, T. Bocklitz, *Biophotonics Translational* **2019**, 1.

[17] B. Gong, L. Shen, C. Chang, S. Zhou, W. Zhou, S. Li, J. Shi, *IEEE 17th International Symposium on Biomedical Imaging (ISBI)*, *IEEE*, Piscataway, NJ, USA **2020**, p. 1106.
[18] Y. Guo, H. Dong, F. Song, C. Zhu, J. Liu, *Image Anal*, *Recognition*, ICIAR **2018**.
[19] B. Xu, J. Liu, X. Hou, B. Liu, J. Garibaldi, I. O. Ellis, A. Green, L. Shen, G. Qiu, *IEEE 16th International Symposium on Biomedical Imaging*, NJ, USA **2019**, p. 914.
[20] S. Saxena, S. Shukla, M. Gyanchandani, *Int. J. Imaging Syst. Technol.* **2020**, *30*, 577.
[21] I. Hirra, M. Ahmad, A. Hussain, M. U. Ashraf, I. A. Saeed, S. F. Qadri, A. M. Alghamdi, A. S. Alfakeeh, *IEEE Access* **2021**, *9*, 24273.
[22] W. A. Wells, X. Wang, C. P. Daghlian, K. D. Paulsen, B. W. Pogue, *Anal. Quant. Cytol. Histol.* **2009**, 197.
[23] M. Z. Alom, C. Yakopcic, M. S. Nasrin, T. M. Taha, V. K. Asari, *J. Digital Imag.* **2019**, *32*, 605.
[24] S. S. Yadav, S. M. Jadhav, *J. Big Data* **2019**, *6*.
[25] F. Shahidi, S. Mohd Daud, H. Abas, N. A. Ahmad, N. Maarop, *IEEE Access* **2020**, *8*, 187531.
[26] M. Peikari, M. J. Gangeh, J. Zubovits, G. Clarke, A. L. Martel, *IEEE Trans Med. Imag.* **2016**, *35*, 307.

How to cite this article: L. Thomas, M. K. Sheeja, *J. Biophotonics* **2023**, e202200359. https://doi.org/10.1002/jbio.202200359